Dual Reactivity Mode of Vinyl Ethylene Carbonates with Anilines: A Catalyst-Controlled Chemodivergent Entry to *N*-Heterocycles and the Observation of Unusual Competing Pathways

Santosh Kumar Keshri[a] and Manmohan Kapur [a,*]

[a]Department of Chemistry, Indian Institute of Science Education and Research Bhopal, Bhopal Bypass Road, Bhauri, Bhopal, 462066, MP, India.

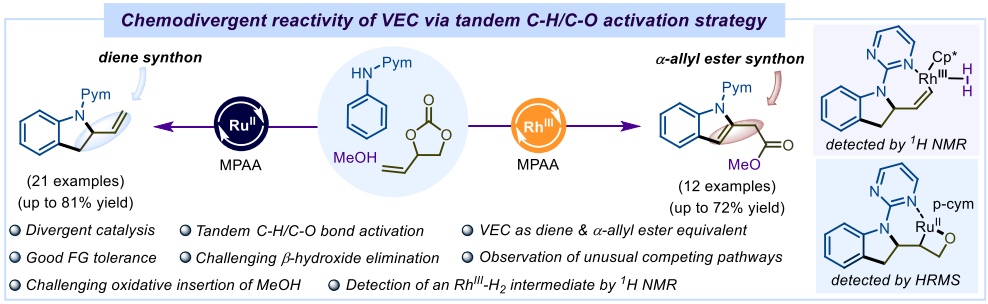

ABSTRACT: A unique catalyst-controlled chemodivergent strategy to access 2-vinyl indolines and indole-2-acetates by overcoming the usual allylic reactivity of vinyl ethylene carbonates (VECs) *via* a tandem C–H/C–O bond activation sequence is disclosed herein. This methodology provides useful molecular scaffolds by following two distinct pathways in a highly step- and atom-economical manner. The pathway features a challenging β-hydroxide elimination and in the Rh-catalyzed transformation, we have observed unusual competing pathways such as an oxidative insertion of MeOH into Rh(III) to give a putative Rh(V)–H intermediate. Mechanistic insights unveil a new reactivity mode of vinyl ethylene carbonates and open a new avenue for divergent catalysis. Post synthetic modification of the annulated products add additional advantage to the methodology.

The challenge of synthesizing divergent scaffolds from simple and readily available starting materials has resulted in transition metal catalyzed C(sp^2)–H functionalization developing as a powerful approach over the last two decades.[1-2] To accomplish this target, the development of novel and methodical strategies, including catalyst-controlled,[3] directing group (DG)-enabled,[4] or manipulating the reaction parameters[5] to modify either chemo-, regio-, or stereoselectivity has become increasingly better understood in recent times. In this context, a coalescence of DG-assisted C(sp^2)–H allylation and intramolecular annulation has proved to be one of the promising solutions for the direct access to privileged structural motifs.[6]

As a smart organic synthon, cyclic carbonates (bearing a native functional group) have attracted increasing attention in several catalytic transformations *via* strain-release-driven decarboxylative ring-opening processes.[7] Among cyclic carbonates, the reactivity of vinyl ethylene carbonates (VECs) have been well studied, leading to the development of various cycloaddition[8] and allylic substitution reactions.[9] The dual reactivity mode of VECs can be envisioned *via* decarboxylative ring opening transformations as triggered by an external promoter leading to the generation of: (i) diene synthon and/or (ii) α-allyl ester synthon which subsequently results in the formation of the coupling product (Scheme 1a). Notably, VECs as a diene equivalent in catalytic reactions remain less explored whereas their reactivity mode as an α-allyl ester equivalent remains elusive till date (Scheme 1a). This unusual reactivity mode of VECs has garnered considerable attention of synthetic organic chemists and these have been utilized as a reactive coupling partner in catalytic organic transformations leading to the formation of important molecular frameworks including heterocycles *via* the formation of chelated metallacyclic intermediates (Scheme 1b). In addition, VECs have been demonstrated to act as a transmuted allyl source to enable TM-catalyzed C–H allylation of arenes through β-oxygen elimination leading to the formation of linear allylated arenes **II** (Scheme 1c, Step-I).[10] Despite impressive research in the area of VECs, it is observed that accessing annulated products in a one pot fashion by employing a single catalytic system is quite challenging and remains rather underexplored (Scheme 1c). In this context, in 2014, Wang and co-workers reported a tandem catalytic system (Rh(III)/Pd(II)) that provided rapid access to vinyl-substituted

Scheme 1. Divergent Reactivity Profile of Vinyl Ethylene Carbonates with Arenes *via* tandem C–H/C–O activation sequence

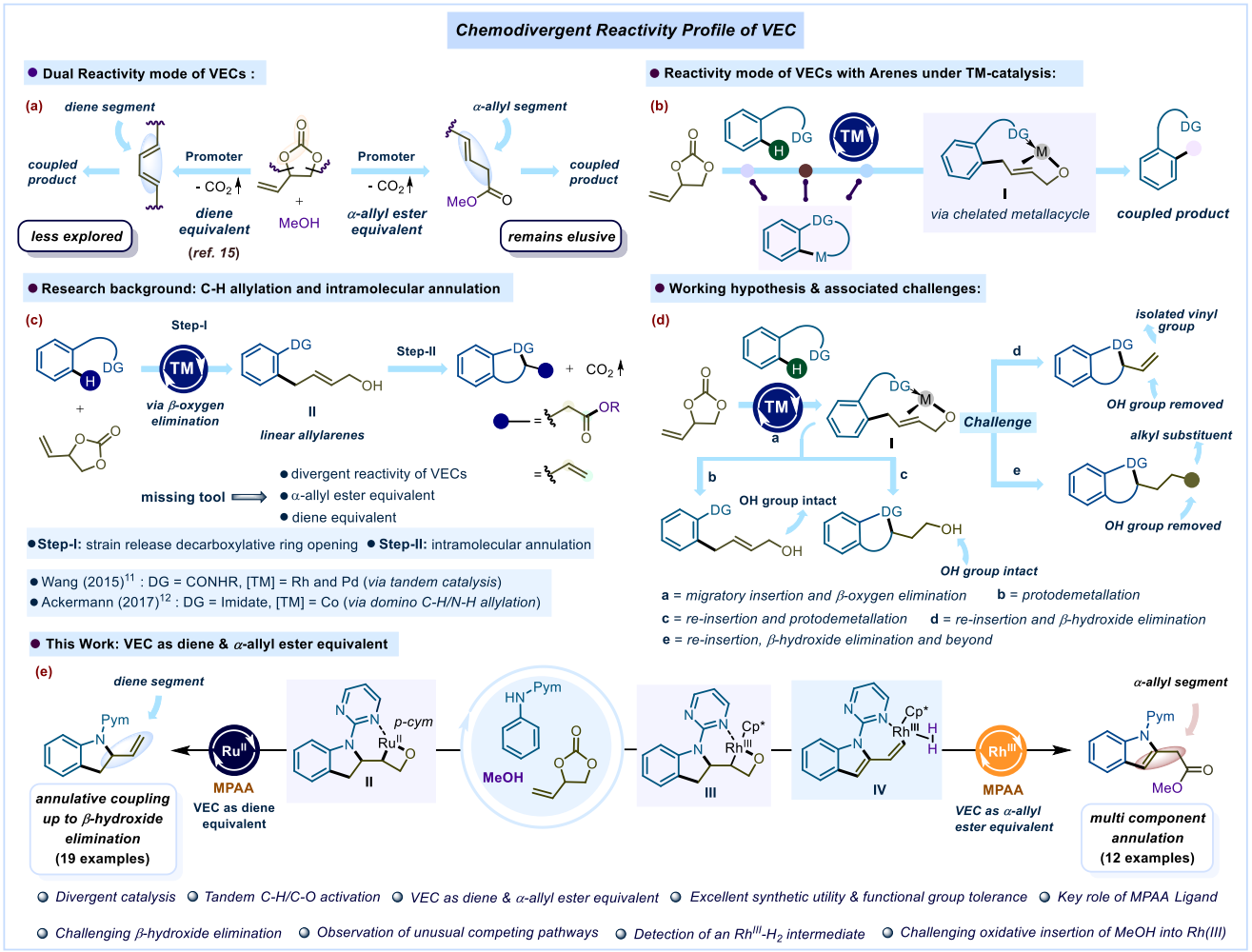

5,6-dihydropyridin-2(1H)-ones and 3,4-dihydroisoquinolin-1(2H)-ones while employing VECs (Scheme 1c).[11] The alkene effect was found to be the key factor for the success of the reaction. In 2017, Ackermann and co-workers used VECs to achieve a domino C–H/N–H allylation to access vinylated heterocycles under Co(III)-catalysis (Scheme 1c).[12] There are critical challenges that need to be considered during coupling of VECs with arenes. After the formation of the crucial metallacyclic intermediate **I** *via* migratory insertion and *β*-oxygen elimination sequence (Scheme 1(d), a), a variety of pathways could result: (i) It may result in the formation of linear allylated arene in which the -OH group remains intact after protodemetallation (Scheme 1(d), b); (ii) Re-insertion of the metal into the 'C=C' bond of the allyl arene followed by protodemetallation may give the annulated product with the terminal -OH group (Scheme 1(d), c); (iii) Intermediate **I** may also lead to the formation of annulated product containing the isolated vinyl group after metal re-insertion and *β*-hydroxide elimination sequence thereafter, bypassing the protodemetallation step, which is synthetically challenging (Scheme 1(d), d); (iv) The resulting annulated product with the vinyl substituent may also react further leading to complex molecular scaffolds and this demands proper designing of substrates or reaction conditions and remains rather underexplored till date (Scheme 1(d), e).

In this work, we describe a catalyst-controlled divergent reactivity profile of vinyl ethylene carbonates (VECs) with anilines,[13] leading to the formation of synthetically challenging 2-vinyl indolines[14] under a Ru(II)/MPAA catalytic system wherein the VEC acts as a diene equivalent,[15] involving a *β*-hydroxide elimination as the key step (Scheme 1e). On the other hand, under Rh(III)/MPAA catalysis, VEC in combination with MeOH was found to act as an *α*-allyl ester equivalent[16] to deliver C2-substituted indoles[17] (Scheme 1d). In this case, a unique reactivity of VEC was observed, extending beyond the *β*-hydroxide elimination step.

The investigations were initiated by reacting *N*-pyrimidyl aniline **1** and 4-vinyl-1,3-dioxolan-2-one **2** under Ru(II) catalysis (Table 1). To our delight, the desired target compound 2-vinyl indoline **3** was chemoselectivity achieved. Encouraged by this important outcome, further optimization led to the desired product with improved yields and after screening several reaction conditions, we concluded that $[Ru(p\text{-}cym)Cl_2]_2$ (5 mol%), $AgSbF_6$ (10 mol%), *N*-Ac-Gly-OH (20 mol%) and PivOH (1.5 equiv.) in MeOH at 80 °C for 24 h was the optimum condition for the best yields of the corresponding 2-vinyl indoline **3** (Table 1) (for a detailed optimization table, see the SI). Replacing the Ru-catalyst with the Rh-catalyst hampered the desired chemoselectivity (Table **1**, entry **2**). Using $AgNTf_2$ instead of $AgSbF_6$ as the additive resulted in reduced yield of the desired product (Table

1, entry **3**). Notably, the efficiency of the reaction was significantly amplified by MPAA ligands (see the SI for details) and was optimal for *N*-Ac-Gly-OH (Table **1**, entry **4**). MPAA ligands play a crucial role by acting as a proton acceptor in the C–H activation step and facilitate the C–H bond cleavage by forming MPAA-bridged binuclear metal complexes.[18]

Table 1. Optimization of Reaction Conditions for Ru-catalysis:

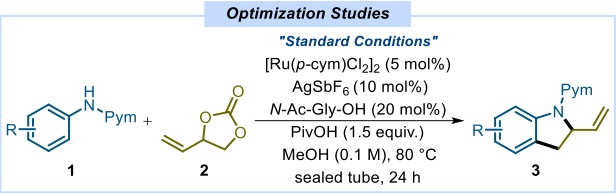

Entry	Deviation from standard conditions	Yield (%)[a]
1	none	66
2	$[Cp^*RhCl_2]_2$ instead of $[Ru(p\text{-cym})Cl_2]_2$	nd
3	$AgNTf_2$ instead of $AgSbF_6$	46
4	Piv-Gly-OH instead of *N*-Ac-Gly-OH	trace
5	$NaOPiv.H_2O$ instead of PivOH	nd
6	$Cu(OAc)_2.H_2O$ instead of PivOH	20
7	AcOH instead of PivOH	45
8	$MesCO_2H$ instead of PivOH	51
9	DCE or 1,4-Dioxane instead of MeOH	trace
10	25 °C/120 °C instead of 80 °C	trace
11	2 mol% of $[Ru(p\text{-cym})Cl_2]_2$ instead of 5 mol%	40

[a]Isolated yields.

Several other additives were tested, and it was found that PivOH was the best amongst the ones scanned (Table **1**, entries **5, 6, 7, 8**). The desired product formation was not observed when the reaction was carried out in other polar aprotic solvents (Table **1**, entry **9**). Only a trace amount of product was detected when the temperature was reduced to 25 °C or increased to 120 °C (Table **1**, entry **10**). Reducing the catalyst loading resulted in a poor outcome (Table **1**, entry **11**).

In the Rh-catalyzed transformation, we observed that the reactivity was not limited up to the indoline formation step rather it extended further to deliver indole-2-acetates **4** through a three-component coupling (Table 2). The formation of functionalized indoles **4** was found to work best under the following conditions: $[Cp^*RhCl_2]_2$ (2 mol %), $AgSbF_6$ (20 mol%), *N*-Ac-Gly-OH (20 mol%), $Cu(OAc)_2{\cdot}H_2O$ (1.0 equiv.) in MeOH at 80 °C for 24 h (Table 2, entry **1**). Here too, the reaction efficiency was sensitive towards catalyst and the additives (Table 2, entry **2, 3**) and was amplified by the MPAA ligand (Table 2, entry **4**). The reaction efficiency further improved by adding the Cu-additive in a proper stoichiometry (Table 2, entry **5, 6**). Other Brønsted acid additives resulted in poor outcomes (Table **2**, entry **7**). It should be noted that solvents other than MeOH did not respond under the optimized conditions (Table **2**, entry **8**). This protocol was sensitive towards temperature, and it was found that 80 °C was optimal for this reaction condition (Table **2**, entry **9**). The yield of the indole-2-acetate decreased upon increasing the loading of the catalyst (Table **2**, entry **10**) (for a detailed optimization table, see the SI).

Table 2. Optimization of Reaction Conditions for Rh-catalysis:

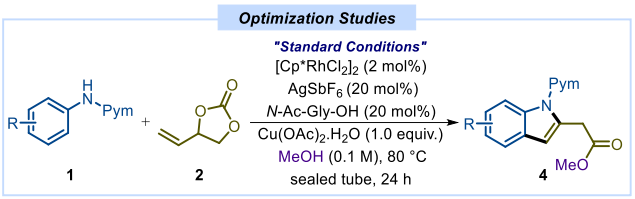

Entry	Deviation from standard conditions	Yield (%)[a]
1	none	72
2	$[Ru(p\text{-cym})Cl_2]_2$ instead of $[Cp^*RhCl_2]_2$	nd
3	$AgNTf_2$ instead of $AgSbF_6$	52
4	Without *N*-Ac-Gly-OH	40
5	2.0 equiv. of $Cu(OAc)_2.H_2O$	59
6	Without $Cu(OAc)_2.H_2O$	nd
7	AcOH/PivOH instead of $Cu(OAc)_2.H_2O$	nd
8	^{t}BuOH/DCE instead of MeOH	nd
9	25 °C/120 °C instead of 80 °C	trace
10	5 mol% of $[Cp^*RhCl_2]_2$ instead of 2 mol%	50

[a]Isolated yields.

With the optimized conditions established, we then probed the reaction scope to explore the versatility of the transformation under Ru-catalysis. The reaction was compatible with most of the anilines screened with excellent chemo- and regioselectivity and demonstrated good functional group tolerance. Various electronic and steric parameters were examined at *ortho*-, *meta*- & *para*-positions of the aryl ring of *N*-pyrimidyl anilines delivering vinyl substituted indolines in moderate to good yields (**3a**–**3s**, Scheme 2a). Notably, the 2,4-disubstituted aniline reacted best under the optimized reaction conditions gave 81% yield of the desired indoline (**3a**, Scheme 2a). The reaction was compatible with a variety of electron-donating and electron-withdrawing substituents including halogens at *para*- and *meta*-positions of the aryl ring of *N*-pyrimidyl anilines, yielding the desired indolines in good yields (**3b**–**3e, 3h, 3i, 3j,** Scheme 2a). Importantly, electron-withdrawing functional groups (-OCF_3, -CO_2Et, -SO_2Me) were well tolerated in this protocol and gave the corresponding products with excellent chemoselectivity (**3f**, **3g, 3k,** Scheme 2a). The chemoselectivity was also retained in the case of polycyclic systems to afford the desired indolines in good yields (**3l**–**3n**, Scheme 2a). The structure of the indoline product was confirmed unambiguously by X-ray crystallographic analysis of **3i**, Scheme 2a). Importantly, the compatibility of the present transformation was further showcased by other directing groups to deliver the products with acceptable yields (**3o**–**3s**, Scheme 2a). Notably, *N*-phenyl acetamide remained unreacted under the standard reaction conditions (**3t**, Scheme 2a).

We next sought to probe the scope and generality of the Rh-catalysis by testing a range of substituted anilines with varied electronic and steric substituents at the aryl ring of the

N-pyridyl anilines (**4a**–**4d**, Scheme 2b). This protocol was compatible with halogens (-Br, -Cl) at different positions of the aryl ring and provided ample opportunity for post-synthetic modifications (**4c**, **4f**, **4j**, Scheme 2b). This methodology was also applied on a polycyclic system to yield the benzo-fused indole-2-acetate in acceptable yields (**4e**, Scheme 3). The reaction worked well with the assistance of pyrimidyl and acetyl directing groups also (**4g–4l**, Scheme 2b). The structure of the indole-2-acetate was confirmed unambiguously by X-ray crystallographic analysis of **4f** (Scheme 2b).

We then moved on to check the utility of the present transformation. Indolines (**3**) reacted with MeOH to afford indole-2-acetates (**4**) in moderate to good yields under oxidative conditions (**4g**, **4a**, **4b**, **4i,** Scheme 3A). To further showcase the importance of the DG in the products, regioselective C7-functionalizations were carried out (Scheme 3B, 3C). Regioselective C7-thiolation[19] and amidation[20] were carried out to deliver **6c** and **8c** respectively in good yields (Scheme 3B, 3C). Chemoselective reductions were also carried out by using the indoline **3c** and indole-2-acetate **4a**. Hydrogenation of **3c** yielded 2-ethyl indoline **9c** in 78% yield (Scheme 3D (a)). Synthesis of 2-hydroxyethyl indole **10a** was carried out by selectively reducing the ester group of **4a** (Scheme 3D (b)).

Next, to gain insights into the pathway of the transformations, detailed mechanistic investigations were carried out (Scheme 4). To check the reversibility of C–H metalation under Ru-catalysis, with added D_2O, in the absence of coupling partner **2**, 75% D incorporation was observed at the *ortho*-position of the recovered starting material (10% consumption of the SM, Scheme 4A (a)). When the study was carried out in the presence of the coupling partner **2**, 70% deuteration was observed at the *ortho*-position of the recovered starting material (Scheme 4A (a)). A significant amount of deuteration was also observed (80% D incorporation without **2** & 40% D with **2**), when we tested the reversibility of the C–H metalation step under Rh-catalysis (Scheme 4A (b))

Scheme 2. Scope of 2-vinyl indolines & indole esters:

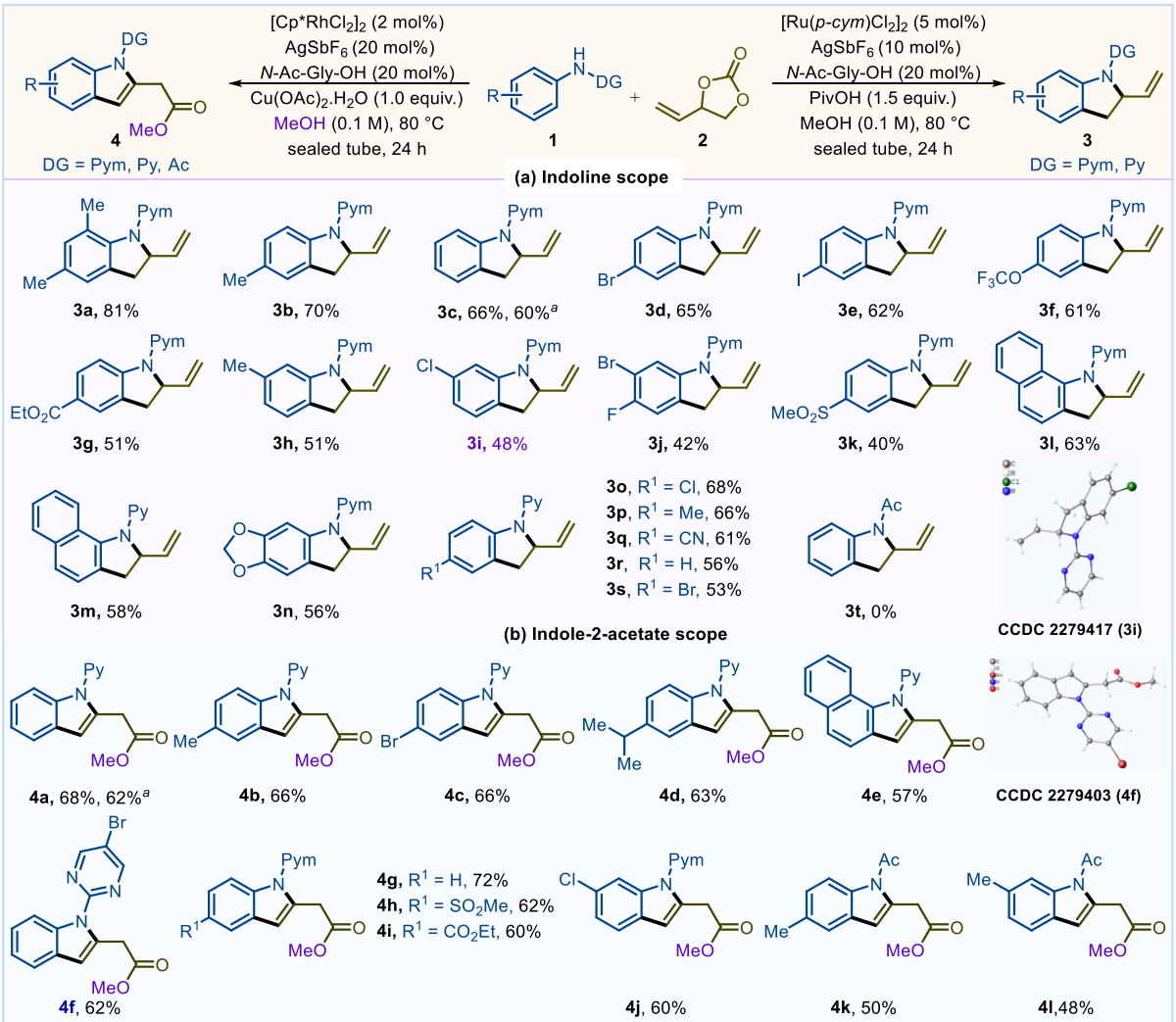

[a]Reaction performed on 1 mmol scale.

Scheme 3. Synthetic Transformations:

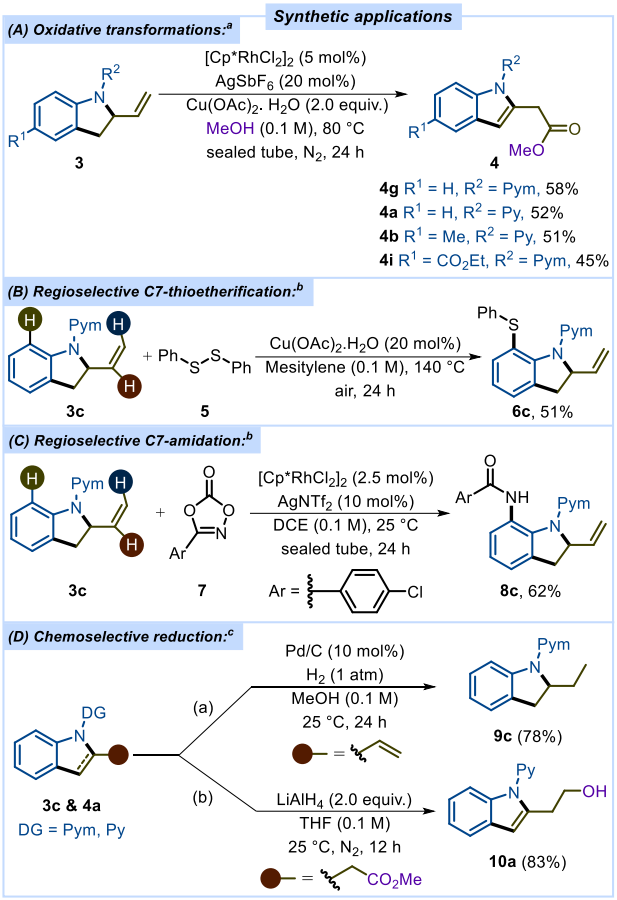

A considerable amount of D to H exchange was also observed under both, Ru-catalysis (93% D to 17% D) (Scheme 4A (c)) as well as [Rh]-catalysis (93% D to 4% D) (Scheme 4A (d)). Owing to the high reversibility of the C–H metallation, reliable results were not obtained when we performed studies to check for a KIE in the C–H activation step under both catalytic conditions.[3c] Additionally, in the conversion of **3** to **4** under Rh-catalysis, the C–H metallation step was found to be mildly reversible indicating that the subsequent steps were faster rather than the reverse step (Scheme 4A (e)).

To probe the origin of chemoselectivity in indoline and indole-2-acetate formation, control experiments were performed by using the pre-formed indoline **3c** (Scheme 5A). Deviation from the standard conditions resulted in a poor outcome. Further, to check the necessity of the MPAA ligand in the conversion of **3** to **4**, the reaction was carried out in the absence of MPAA ligand, and the reaction proceeded smoothly which implies that the MPAA ligand has a significant role only up to the indoline formation and may not be involved in the formation of the indole-2-acetate **4** (Scheme 5A, entry 3). Notably, it was found that the $Cu(OAc)_2.H_2O$ additive has a significant role in the indole-2-acetate formation (Scheme 5A, entry 4). This may be due to the fact that the copper additive plays a key role in the oxidation step to give the final product **4**. Polar protic solvents other than MeOH did not yield the desired product (Scheme 5A, entry 5). It is also imperative to note that the reactivity of VEC was restricted under Ru-catalysis up to the indoline formation under the standard reaction conditions and did not proceed further to yield the indole-2-acetate (Scheme 5A, entry 6).

Scheme 4. Mechanistic Investigations-I:

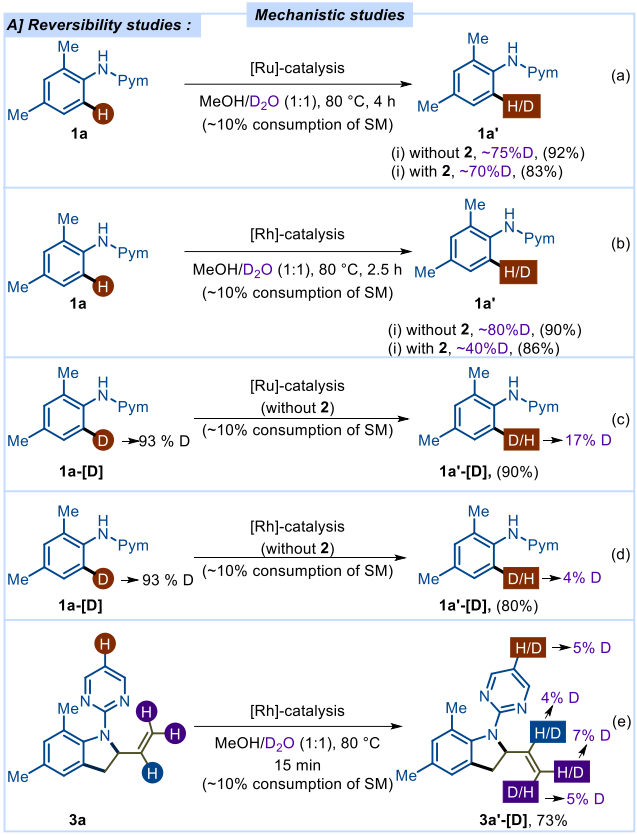

While a mechanism for the Ru-catalyzed formation of the indoline could be predicted based on the mechanistic studies and literature precedent, it was the formation of the indole-2-acetates that intrigued us the most. Therefore, we moved on to check the mechanism of MeOH incorporation in the formation of indole-2-acetate **4**. We reacted **3a** with $[Cp^*RhCl_2]_2$ (10 mol%), $AgSbF_6$ (20 mol%) in presence of anhyd. NaOAc (1.0 equiv.) as an additive in CD_3OD (0.1 M) at 80 °C and followed the reaction by ^1H NMR (Scheme 5B). The ^1H NMR spectrum of the reaction mixture showed a characteristic triplet in the upfield region at −8.71 ppm (J = 29 Hz), indicating the presence of a Rh(III)–H_2 species.[21] Additionally, two organometallic intermediates (Rh(V)-H and Rh(V)-D) were detected by ESI-HRMS analysis (Scheme 5C, 5D, also see the SI for further details). To confirm this observation, a spike test was also performed where the NMR tube containing the reaction mixture was bubbled with H_2 gas. The characteristic peak for H_2 was observed at δ ~4.62 ppm which further confirmed the release of H_2 gas in the reaction aliquot during the progress of the reaction (see SI for further details). These results seemed to indicate that MeOH gets oxidatively inserted into Rh(III)-species[22] to form a putative Rh(V)–H species.[23] This observation is rather surprising, since to the best of our knowledge, such oxidative insertions into the O–H bond of alcohols are known in literature mostly with low-valent metal complexes.[24] Additionally, to confirm the role of the MPAA ligand in C–H activation under both Ru- and Rh-catalysis, mass spectrometry studies were carried out (Scheme 5E (i), (ii)).

https://doi.org/10.26434/chemrxiv-2024-cwphv **ORCID:** https://orcid.org/0000-0003-2592-6726

Scheme 5. Mechanistic Investigations-II:

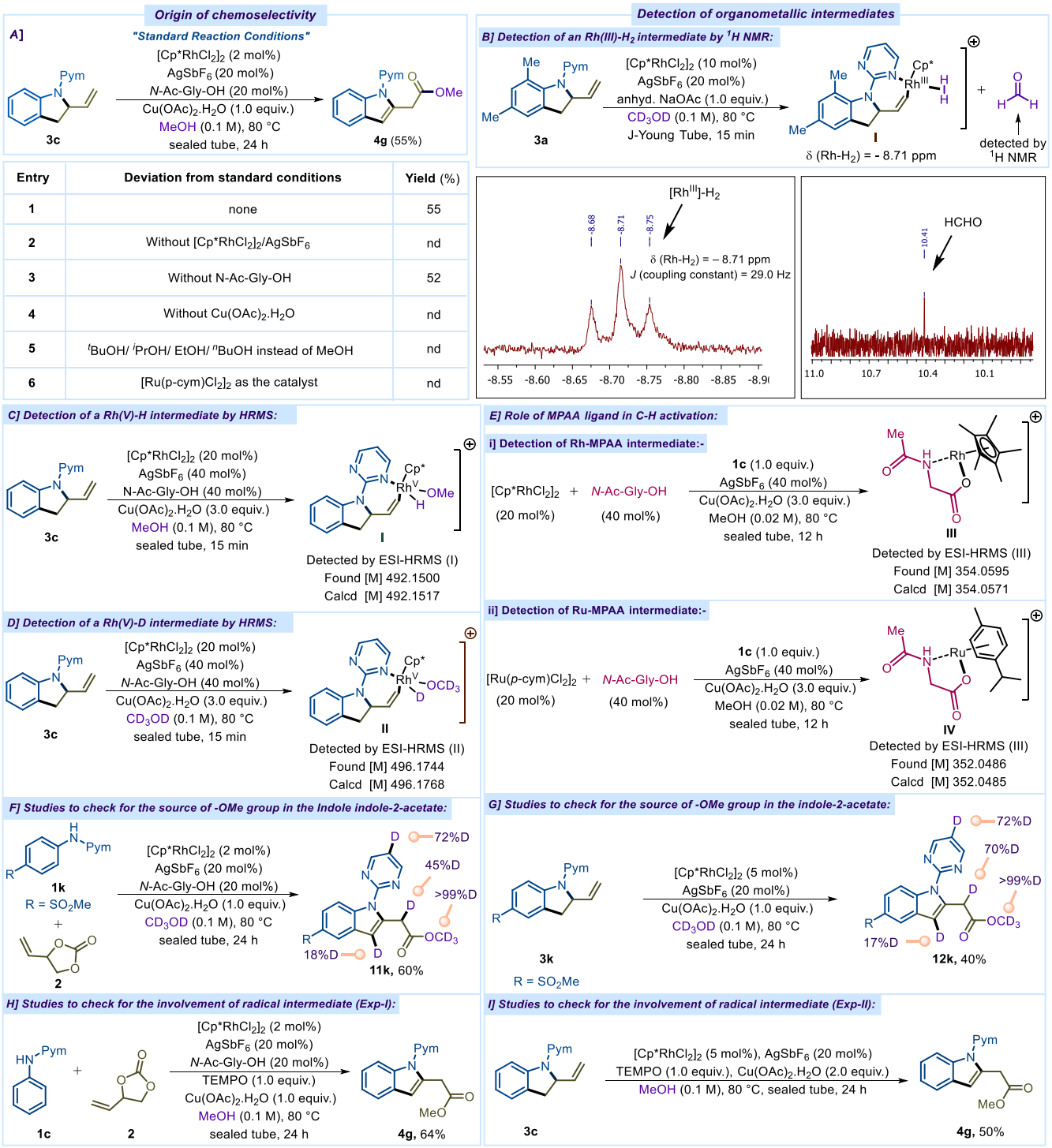

Entry	Deviation from standard conditions	Yield (%)
1	none	55
2	Without $[Cp^*RhCl_2]_2$/$AgSbF_6$	nd
3	Without N-Ac-Gly-OH	52
4	Without $Cu(OAc)_2.H_2O$	nd
5	^{t}BuOH/ ^{i}PrOH/ EtOH/ ^{n}BuOH instead of MeOH	nd
6	$[Ru(p\text{-}cym)Cl_2]_2$ as the catalyst	nd

The generation of the Rh-MPAA complex **III** was confirmed by reacting **1c** with $[Cp^*RhCl_2]_2$ (20 mol%), *N*-Ac-Gly-OH (40 mol%) in presence of $AgSbF_6$ (40 mol%) and $Cu(OAc)_2.H_2O$ (3.0 equiv.) as an additive in MeOH (0.02 M) at 80 °C and by following the reaction by HRMS analysis (Scheme 5E (i)). Similarly, the generation of Ru-MPAA complex **IV** was also examined and ESI-HRMS indicated the formation of the Ru–MPAA species during the reaction (Scheme 5E (ii)). To further confirm the source of the -OMe group in the indole-2-acetate, reactions were carried out by using **1k** and **3k** under the standard Rh-catalysis by using CD_3OD (0.1 M) (Scheme 5F, 5G). Expectedly, we observed deuterium as well as $-OCD_3$ incorporation in the products **11k** and **12k**. Further, to check for the involvement of single electron transfer pathways in the indole-2-acetate formation, two different reactions were carried out by using TEMPO as radical quencher under the standard Rh-catalysis conditions (Scheme 5H, 5I). The formation of indole-2-acetate **4g** in good yields confirmed that the reaction did not

proceed through a SET pathway in any of the intermediate steps of the catalytic cycle.

Based on the aforementioned control experiments, mechanistic studies and previous literature reports,[10-12] a plausible mechanism for the Ru-catalyzed indoline formation is depicted in Scheme 6. The reaction was initiated with the formation of active Ru(II) species **I**. Next, a chelation assisted, directed and reversible *ortho*- C–H activation results in the formation of cationic intermediate **II** (Scheme 6). Coordination, regioselective migratory insertion (*via* a [6,4]-fused ruthenacycle **III)**, *β*-oxygen elimination[10] and subsequent regioselective re-insertion of N–Ru bond[3c] into the internal olefinic double bond of intermediate **IV** delivers the key intermediate **V** (Scheme 6). Finally, a *β*-hydroxide elimination[26] from **V** releases the desired indoline **3c** and regenerates the Ru-catalyst *via* an active [Ru]-OH species **VI**. Notably, the intermediates **I**, **II, V** and **VI** were detected in ESI-HRMS (see the SI for details).

Scheme 6. Ru-catalytic cycle:

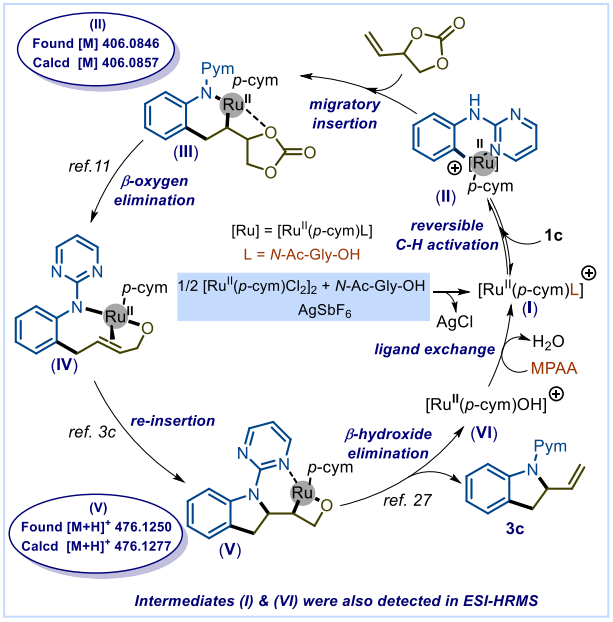

Multiple pathways can be proposed for the Rh-catalyzed indole-2-acetate formation. To begin with, the *in-situ* generated active Rh-catalyst **I** engages in a reversible C–H activation to give the intermediate **II** (Scheme 7). Further, coordination, regioselective migratory insertion and subsequent *β*-oxygen elimination delivers the chelated organometallic species **IV** *via* a [6,4]-fused intermediate **III**. It subsequently undergoes regioselective re-insertion of the Rh-species[3c, 25] followed by a *β*-hydroxide elimination[26] to regenerate the active catalyst **I** *via* **VI** along with the release of intermediate **VII** (Scheme 7). This intermediate **VII** can undergo a regioselective re-insertion of the [Rh]-intermediate **VIII** (generated *in situ* from **VI** through ligand exchange with [Cu]) to give a thermodynamically more stable intermediate **X** (following **path a**). Species **X** may undergo a facile oxidative insertion with MeOH[22] to form the putative [Rh(V)]-H species[23] **XI** as confirmed by ^{1}H NMR and ESI-HRMS analysis. This was also confirmed by the detection of the D-[Rh]-species in ESI-HRMS and other control experiments (Scheme 5D, 5F, 5G). Intermediate **XI** may also be formed from **VIII** *via* regioselective C–H activation of indoline **VII** through an oxidative addition mechanism and followed by a ligand exchange with MeOH[23f] (following **path b**).

Scheme 7. Rh-catalytic cycle:

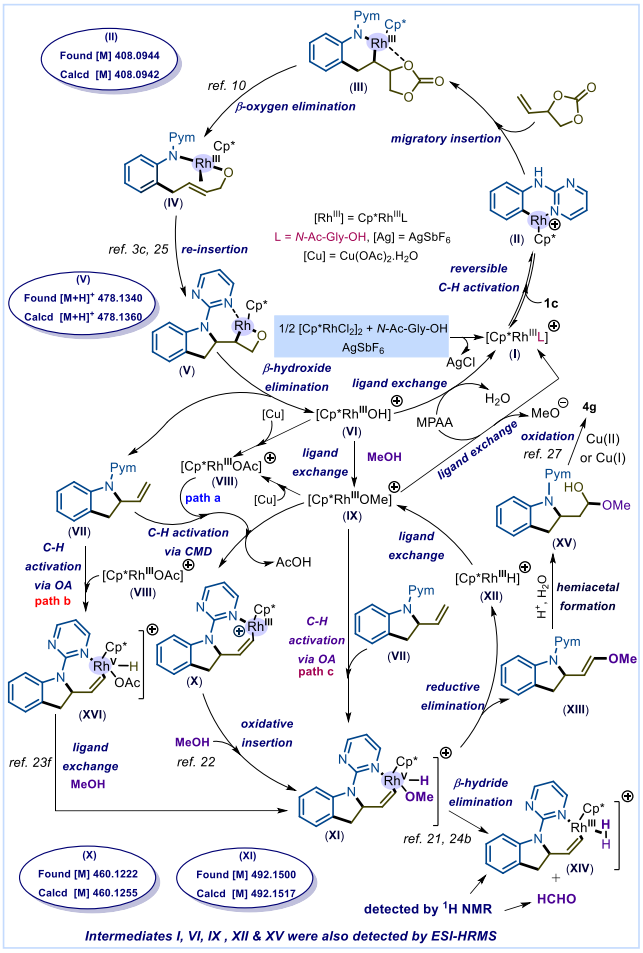

Intermediate **XI** may also be generated from intermediate **IX** (generated from species **VI** *via* ligand exchange with MeOH) after regioselective C–H activation through an oxidative addition mechanism (following **path C**). A fast reductive elimination of species **XI** leads to **XIII** and a subsequent hydrolysis by H^+/H_2O forms the corresponding hemiacetal **XV**. Subsequently, oxidation[27] as assisted by Cu(II) or Cu(I) leads to the formation of the indole-2-acetate **4g**. The active [Rh(III)]-catalyst **IX** is regenerated from the Cp*Rh(III)-H species **XII**. The intermediate **IX** subsequently undergoes ligand exchange with MPAA to regenerate species **I** and continue the catalytic cycle (Scheme 7). In this case too, the intermediates **I**, **II**, **V**, **VI**, **IX**, **X**, **XI, XII and XV** were detected in ESI-HRMS. Additionally, intermediate **XI** may generate the putative Rh(III)-H_2 species[21, 24b] **XIV** along with the release of HCHO (as detected by ^{1}H NMR studies, Scheme 5B) *via* *β*-hydride elimination pathway. At this moment it is rather difficult to confirm what would be the preferred pathway for the transformation, especially since all three pathways involve a high-valent Rh(V) species. Further studies in this regard are in progress.

To conclude, we have developed a strain-release-driven dual reactivity pattern of VECs *via* a tandem C–H/C–O activation sequence to access synthetically useful scaffolds in highly atom- and step-economical manner. Its reactivity as diene synthon in Ru-catalysis had been unexplored and as an α-allyl ester equivalent in Rh-catalysis remained elusive and this is highlighted successfully in our methodology. Additionally, detailed mechanistic insights reveal an interesting mechanistic picture involving unusual competing pathways in the Rh-catalysis. Post synthetic modifications of the annulated products has added additional advantages to this protocol.

ASSOCIATED CONTENT

Supporting information includes experimental details and spectral data of all new compounds, X-ray data of 3i, 4g.

AUTHOR INFORMATION

Corresponding Author

Manmohan Kapur- *Department of Chemistry, Indian Institute of Science Education and Research Bhopal, Bhopal 462066 MP, India;* Email: mk@iiserb.ac.in

Authors

Santosh Kumar Keshri- *Department of Chemistry, Indian Institute of Science Education and Research Bhopal, Bhopal 462066 MP, India*

Notes

The authors declare no competing financial interest.

ACKNOWLEDGMENT

Funding from SERB-India (STR/2019/000072) is gratefully acknowledged. S.K.K. thanks CSIR-India for a research fellowship. We thank Dr. Pirudhan Karak (IISERB) for the assistance with X-ray analysis and CIF, IISERB for the analytical data (NMR, MS and XRD). We also thank the Director, IISERB, for funding and infrastructural facilities.

REFERENCES

(1) (a) Hartwig, J. F. *Organotransition Metal Chemistry: From Bonding to Catalysis;* University Science Books: **2010**. (b) Crawley, M. L; Trost, B. M.; Shen, H. C. *Selected Applications of Transition Metal-Catalyzed Carbon–Carbon Cross-Coupling Reactions in the Pharmaceutical Industry; Wiley-VCH: Weinheim*, **2012**. (c) Johansson Seechurn, C. C. C.; Kitching, M. O.; Colacot, T. J.; Snieckus, V. Palladium-Catalyzed Cross-Coupling: A Historical Contextual Perspective to the 2010 Nobel Prize. *Angew. Chem., Int. Ed.* **2012**, *51*, 5062.
(2) For recently selected reviews, see: (a) Abrams, D. J.; Provencher, P. A.; Sorensen, E. J. Recent Applications of C–H Functionalization in complex natural product synthesis. *Chem. Soc. Rev.* **2018**, *47*, 8925. (b) Saint-Denis, T. G.; Zhu, R.-Y.; Chen, G.; Wu, Q.-F.; Yu, J.- Q. Enantioselective C(sp^3)–H bond activation by chiral transition-metal-catalysts. *Science* **2018**, *359*, eaao4798. (c) Gandeepan, P.; Müller, T.; Zell, D.; Cera, G.; Warratz, S.; Ackermann, L. 3d Transition Metals for C–H Activation. *Chem. Rev.* **2019**, *119*, 2192. (d) Rogge, T.; Kaplaneris, N.; Chatani, N.; Kim, J.; Chang, S.; Punji, B.; Schafer, L. L.; Musaev, D. G.; Wencel-Delord, J.; Roberts, C. A.; Sarpong, R.; Wilson, Z. E.; Brimble, M. A.; Johansson, M. J.; Ackermann, L. C–H activation. *Nat. Rev. Methods Primers* **2021**, *1*, 43. (e) Liu B., Yang, L.; Li, P.; Wang F.; Li, X. Recent advances in transition-metal-catalyzed olefinic C–H functionalization. *Org. Chem. Front.* **2021**, *8*, 1085. (f) Kumar, P.; Nagtilak, P. J.; Kapur, M. Transition Metal-Catalyzed C–H functionalizations of Indoles. *New J. Chem.* **2021**, *45*, 13692. (g) Rej, S.; Das, A.; Chatani, N. Strategic evolution in transition metal-catalyzed directed C–H bond activation and future directions. *Coord. Chem. Rev*. **2021**, *431*, 213683. (h) Dalton, T.; Faber T.; Glorius, F. C–H Activation: Toward Sustainability and Applications. *ACS Cent. Sci.* **2021**, *7*, 245.
(3) (a) Das, R.; Khot, N. K.; Deshpande, A. S.; Kapur, M. Catalyst-control in Switching the Site-Selectivity of C–H Olefinations of 1,2-dihydroquinolines: An Approach to Positional-selective Functionalization of Quinolines. *Chem. Eur. J.* **2020**, *26*, 927. (b) Wu, X.; Witzig, R. M.; Beaud, R.; Fischer, C.; Haussinger, D.; Sparr, C. Catalyst Control Over Sixfold Stereogenicity. *Nature Catalysis*, **2021**, *4*, 457. (c) Keshri, S. K.; Madhavan, S.; Kapur, M. Catalyst-Controlled Chemodivergent Reactivity of Vinyl Cyclopropanes: A Selective Approach Toward Indoles and Aniline Derivatives. *Org. lett.* **2022**, *24*, 9043.
(4) (a) Yang, K.; Song, M.; Liu, H.; Ge, H. Palladium-catalyzed direct asymmetric C–H bond functionalization enabled by the directing group strategy. *Chem. Sci.* **2020**, *11*, 12616. (a) Jeon, J.; Lee, C.; Park, I.; Hong, S. Regio- and Stereoselective Functionalization Enabled by Bidentate Directing Groups. *Chem. Rec.* **2021**, *21*, 3613.
(5) (a) Yi, W.; Chen, W.; Liu, F.-X.; Zhong, Y.; Wu, D.; Zhou, Z.; Gao, H. Rh(III)-Catalyzed and Solvent-Controlled Chemoselective Synthesis of Chalcone and Benzofuran Frameworks *via* Synergistic Dual Directing Groups Enabled Regioselective C–H Functionalization: A Combined Experimental and Computational Study. *ACS Catal.* **2018**, *8*, 9508. (b) Zhao, F.; Gong, X.; Lu, Y.; Qiao, J.; Jia, X.; Ni, H.; Wu, X.; Zhang X. Additive-Controlled Divergent Synthesis of Tetrasubstituted 1,3-Enynes and Alkynylated 3*H*-Pyrrolo[1,2-a]indol-3-ones *via* Rhodium Catalysis. *Org. Lett.* **2021**, *23*, 727.
(6) (a) Cai, X.; Song, X.; Yang, X.; Zhang, X.; Fan, X. A divergent construction of fused and bridged carbo-/heterocyclic scaffolds *via* cascade reactions of aryl azomethine imines with vinyl cyclic carbonates. *Org. Chem. Front.* **2023**, *10*, 1015. (b) Min, S.; Kim, T.; Jeong, T.; Yang, J.; Oh, Y.; Moon, K.; Rakshit, A.; Kim, I. S. Synthesis of 2-Formyl Carbazoles *via* Tandem Reaction of Indolyl Nitrones with 2-Methylidene Cyclic Carbonate *Org. Lett.* **2023**, *25*, 4298.
(7) (a) Guo, W.; Gómez, J. E.; Cristofol, A.; Xie, J.; Kleij, A. W. Catalytic Transformations of Functionalized Cyclic Organic Carbonates. *Angew. Chem., Int. Ed.* **2018**, *57*, 13735. (b) Li, Q.-Z.; Guan, Y.-L.; Huang, Q.-W.; Qi, T.; Xiang, P.; Zhang, X.; Leng, H.-J.; Li, J.-L. Temperature-Controlled Divergent Asymmetric Synthesis of Indole-Based Medium-Sized Heterocycles through Palladium Catalysis *ACS Catal.* **2023**, *13*, *2*, 1164.
(8) (a) Khan, I.; Zhao, C.; Zhang, Y. J. Pd-Catalyzed asymmetric decarboxylative cycloaddition of vinylethylene carbonates with 3-cyanochromones *Chem. Commun.* **2018**, *54*, 4708. (b) Zheng, Y.; Qin, T.; Zi, W. Enantioselective Inverse Electron Demand (3 + 2) Cycloaddition of Palladium-Oxyallyl Enabled by a Hydrogen-Bond-Donating Ligand *J. Am. Chem. Soc.* **2021**, *143*, 1038.
(9) (a) Khan, S.; Li, H.; Zhao, C.; Wu, X.; Zhang, Y. J. Asymmetric Allylic Etherification of Vinylethylene Carbonates with Diols *via* Pd/B Cooperative Catalysis: A Route to Chiral Hemi-Crown Ethers. *Org. Lett.* **2019**, *21*, *23*, 9457. (b) Khan, S.; Ahmed, T.; Rasheed, T.; Ullah, T. Recent applications of vinylethylene carbonates in Pd-catalyzed allylic substitution and annulation reactions: Synthesis of multifunctional allylic and cyclic structural motifs. *Coord. Chem. Rev.* **2022**, *462*, 214526.
(10) (a) Zhang, S.-S.; Wu, J.-Q.; Lao, Y.-X.; Liu, X.-G.; Liu, Y.; Lv, W.-X.; Tan, D.-H.; Zeng, Y.-F.; Wang, H. Mild Rhodium(III)-Catalyzed C–H Allylation with 4-Vinyl-1,3-Dioxolan-2-Ones: Direct and Stereoselective Synthesis of (*E*)-Allylic Alcohols. *Org. Lett.* **2014**, *16*, 6412. (b) Sharma, S.; Shin, Y.; Mishra, N. K.; Park, J.; Han, S.; Jeong, T.; Oh, Y.; Lee, Y.; Choi, M.; Kim I. S.; Rhodium-catalyzed mild and selective C–H allylation of indolines and indoles with 4-vinyl-1,3-

dioxolan-2-one: facile access to indolic scaffolds with an allylic alcohol moiety. *Tetrahedron.* **2015**, *71*, 2435. (c) Lu, Q.; Klauck F. J. R.; Glorius, F. Manganese-catalyzed allylation *via* sequential C–H and C–C/C–Het bond activation. *Chem. Sci.* **2017**, *8*, 3379. (d) Wang, H.; Choi, I.; Rogge, T.; Kaplaneris, N.; Ackermann, L. Versatile and robust C–C activation by chelation assisted manganese catalysis. *Nature Catalysis* **2018**, *1*, 993. (e) Ghosh, A. K.; Das, K. K.; Hazra, A. *ortho*-Allylation of 2-Arylindazoles with Vinyl Cyclic Carbonate and Diallyl Carbonate *via* Manganese-Catalyzed C–H Bond Activation. *Adv. Synth. Catal.* **2021**, *363*, 4974.

(11) Zhang, S.-S.; Wu, J.-Q.; Liu, X.; Wang, H. Tandem Catalysis: Rh(III)-Catalyzed C–H Allylation/Pd(II)-Catalyzed *N*-Allylation Toward the Synthesis of Vinyl-Substituted *N*-Heterocycle. *ACS Catal.* **2015**, *5*, 210.

(12) Wang, H.; Lorion, M. M.; Ackermann, L. Domino C–H/N–H Allylation of Imidates by Cobalt Catalysis. *ACS Catal.* **2017**, *7*, 3430.

(13) (a) Rappoport, Z. *The Chemistry of Anilines*; Wiley: **2007**. (b) Ricci, A. *Amino Group Chemistry: From Synthesis to the Life Sciences*; Wiley: **2008**. (c) Tischler, O.; Toth, B.; Novak, Z. Mild Palladium Catalyzed *ortho*-C–H Bond Functionalizations of Aniline Derivatives. *Chem. Rec.* **2017**, *17*, 184. (d) Khake, S. M.; Chatani, N. Rhodium (III)-catalyzed Oxidative C–H alkylation of Aniline Derivatives with Allyl alcochols. *ACS. Catal.* **2022**, *12*, 4394.

(14) (a) Liu, D.; Zhao, G.; Xiang L.; Diverse Strategies for the Synthesis of the Indoline Scaffold. *Eur. J. Org. Chem.* **2010**, 21, 3975. (b) Podoll, J. D.; Liu, Y.; Chang, L.; Walls, S.; Wang, W.; Wang, X. Bio-Inspired Synthesis Yields a Tricyclic Indoline That Selectively Resensitizes Methicillin Resistant Staphylococcus Aureus (MRSA) to *β*-Lactam Antibiotics. *Proc. Natl. Acad. Sci. U. S. A.* **2013**, *110* (*39*), 15573. (c) Park, J.; Mishra, N. K.; Sharma, S.; Han, S.; Shin, Y.; Jeong, T.; Oh, J. S.; Kwak, J. H.; Jung, Y. H.; Kim, I. S. Mild Rh(III)-Catalyzed C7-Allylation of Indolines with Allylic Carbonates. *J. Org. Chem.* **2015**, *80* (*3*), 1818. (d) Pan, C.; Wang, Y.; Wu, C.; Yu, J.-T. Rhodium-Catalyzed C7-Alkylation of Indolines with Maleimides. *Org. Biomol. Chem.* **2018**, *16* (*5*), 693. (e) Banjare, S. K.; Chebolu, R.; Ravikumar, P. C. Cobalt Catalyzed Hydroarylation of Michael Acceptors with Indolines Directed by a Weakly Coordinating Functional Group. *Org. Lett.* **2019**, *21*, 4049.

(15) Xue, S.; Cristo`fol, À.; Limburg, B.; Zeng, Q.; Kleij, A. W. Dual Cobalt/Organophotoredox Catalysis for Diastereo- and Regioselective 1,2-Difunctionalization of 1,3-Diene Surrogates Creating Quaternary Carbon Centers. *ACS Catal.* **2022**, *12*, 3651.

(16) Franckevicius, V.; Cuthbertson, J. D.; Pickworth, M.; Pugh, D. S.; Taylor, R.˘ J. Asymmetric decarboxylative allylation of oxindoles. *Org. Lett.* **2011**, *13*, 4264. (b) Trost, B. M.; Michaelis, D. J.; Charpentier, J.; Xu, J. Palladium-Catalyzed Allylic Alkylation of Carboxylic Acid Derivatives: *N*-Acyloxazolinones as Ester Enolate Equivalents. *Angew. Chem., Int. Ed.* **2012**, *51*, 204. (c) Laidlaw, G.; Franckevicius,˘ V. Palladium-Catalyzed Decarboxylative Asymmetric Allylic Alkylation of Thietane 1,1-Dioxides. *Org. Lett.* **2022**, *24*, 400.

(17) (a) Kochanowska-Karamyan, A. J.; Hamann, M. T. Marine Indole Alkaloids: Potential New Drug Leads for the Control of Depression and Anxiety. *Chem. Rev.* **2010**, *110*, 4489. (b) Kaushik, N. K.; Kaushik, N.; Attri, P.; Kumar, N.; Kim, C. H.; Verma A. K.; Choi, E. H. Biomedical Importance of Indoles. *Molecules*, **2013**, *18*, 6620. (c) Zhang, M.-Z.; Chen, Q.; Yang, G.-F. A review on recent developments of indole-containing antiviral agents. *Eur. J. Med. Chem.* **2015**, *89*, 421. (d) Kumar, P.; Nagtilak, P. J.; Kapur, M. Transition metal-catalyzed C–H functionalizations of Indoles. *New J. Chem.* **2021**, *45*, 13692. (e) Tan, D. X.; Han, F. S.; The Application of C–H bond functionalization in the total syntheses of indole natural products. *Org. Chem. Front.* **2022**, *9*, 1195.

(18) (a) Cheng, G. J.; Yang, Y. F.; Liu, P.; Chen, P.; Sun, T. Y.; Li, G.; Zhang, X.; Houk, K. N.; Yu, J. Q.; Wu, Y. D. Role of *N*-acyl amino acid ligands in Pd(II)-catalyzed remote C–H activation of tethered arenes. *J. Am. Chem. Soc.* **2014**, *136*, 894. (b) Shao, Q.; Wu, K.; Zhuang, Z.; Qian, S.; Yu, J.-Q. From $Pd(OAc)_2$ to Chiral Catalysts: The Discovery and Development of Bifunctional Mono-*N*-Protected Amino Acid Ligands for Diverse C–H Functionalization Reactions. *Acc. Chem. Res.* **2020**, *53*, 833.

(19) Gandeepan, P.; Koeller, J.; Ackermann, L. Expedient C–H Chalcogenation of Indolines and Indoles by Positional-Selective Copper Catalysis. *ACS Catal.* **2017**, *7*, 1030.

(20) Jeon, M.; Mishra, N. K.; De, U.; Sharma, S.; Oh, Y.; Choi, M.; Jo, H.; Sachan, R.; Kim, H. S.; Kim, I. S. Rh(III)-Catalyzed C–H Functionalization of Indolines with Readily Accessible Amidating Reagent: Synthesis, Anticancer Evaluation. *J. Org. Chem.* **2016**, *81*, 9878.

(21) Findlater, M.; Schultz, K. M.; Bernskoetter, W. H.; Cartwright-Sykes, A.; Heinekey, D. M.; Brookhart, M. Dihydrogen Complexes of Iridium and Rhodium. *Inorg. Chem.* **2012**, *51*, 4672.

(22) (a) Li, S.; Cui, W.; Wayland, B. B. Competitive O–H and C–H oxidative addition of CH_3OH to rhodium(II) porphyrins. *Chem. Commun.* **2007**, 4024. (b) Lv, H.; Kang, H.; Zhou, B.; Xue, X.; Engle, K. M.; Zhao, D. Nickel-catalyzed intermolecular oxidative Heck arylation driven by transfer hydrogenation. *Nat. Commun.* **2019**, *10*, 5025.

(23) (a) Giri, R.; Thapa, S.; Kafle, A. Palladium-Catalyzed, Directed C–H Coupling with Organometallics. *Adv. Synth. Catal.* **2014**, *356*, 1395. (b) Sarbajna, A.; Dutta, I.; Daw, P.; Dinda, S.; Rahaman, S. M. W.; Sarkar, A.; Bera, J. K. Catalytic Conversion of Alcohols to Carboxylic Acid Salts and Hydrogen with Alkaline Water. *ACS Catal.* **2017**, *7*, 2786. (c) VásquezCéspedes, S.; Wang, X.; Glorius, F. Plausible Rh(V) Intermediates in Catalytic C–H Activation Reactions. *ACS Catal.* **2018**, *8*, 242. (d) Kumar, A.; Semwal, S.; Choudhury, J. Catalytic Conversion of CO_2 to Formate with Renewable Hydrogen Donors: An Ambient Pressure and H_2-Independent Strategy. *ACS Catal.* **2019**, *9*, 2164. (e) Wagner-Carlberg, N.; Rovis, T. Rhodium (III)-Catalyzed Anti-Markovnikov Hydroamidation of Unactivated Alkenes Using Dioxazolones as Amidating Reagents. *J. Am. Chem. Soc.* **2022**, *144*, 22426. (f) Li, B. W.; Yan, J.; Wang, X.; Yu, X.; Li, X.; Zhang, L. J.; Li, H. Theoretical study on Rh(III)-catalyzed reaction of allenylsilanes with *N*-methoxybenzamides. *J. Organomet. Chem.* **2023**, *984*, 122557.

(24) (a) Blum, O.; Milstein, D. Oxidative Addition of Water and Aliphatic Alcohols by $IrCl(trialkylphosphine)_3$. *J. Am. Chem. Soc.* **2002**, *124*, 11456. (b) Wang, Y.; Huang, Z.; Leng, X.; Zhu, H.; Liu, G.; Huang, Z. Transfer Hydrogenation of Alkenes Using Ethanol Catalyzed by a NCP Pincer Iridium Complex: Scope and Mechanism. *J. Am. Chem. Soc.* **2018**, *140*, 4417. (c) Fang, H.; Shimada, S. Oxidative Addition of Water to Ir(I) Complexes Bearing a Pincer-Type Silyl Ligand. *ACS Omega* **2022**, *7*, *23*, 20237.

(25) (a) Wang, C. Q.; Ye, L.; Feng, C.; Loh, T. P. C–F bond cleavage enabled redox-neutral [4 + 1] annulation *via* C–H bond activation. *J. Am. Chem. Soc.* **2017**, *139*, 1762. (b) Li, Y.; Xu, S. Transition-Metal-Catalyzed C–H Functionalization for Construction of Quaternary Carbon Centers. *Chem. -Eur. J.* **2018**, *24*, 16218.

(26) Kumar, G. S.; Kapur, M. Ruthenium-Catalyzed, Site-Selective C–H Allylation of Indoles with Allyl Alcohols as Coupling Partners. *Org. Lett.* **2016**, *18*, 1112.

(27) (a) Balogh-Hergovich, E.; Speier, G. Kinetics and mechanism of the dehydrogenation of indolines to indoles with dioxygen catalyzed by chloro(pyridine)copper(I) in dichloromethane solution. *J. Mol. Catal.* **1986**, *37*, 309. (b) Allen, S. E.; Walvoord, R. R.; Padilla-Salinas, R.; Kozlowski, M. C. Aerobic Copper-Catalyzed Organic Reactions. *Chem. Rev.* **2013**, *113*, 6234.